Detection of potato beetle damage using remote sensing from small unmanned aircraft systems

E. Raymond Hunt, Jr. [1], Silvia I. Rondon [2], Robert W. Turner [3], Alan E. Bruce [3], and Josh J. Brungardt [4]

[1] Hydrology and Remote Sensing Laboratory, USDA-ARS, Beltsville, MD; [2] Hermiston Agricultural Research and Extension Center, Oregon State University, Hermiston, OR; [3] Boeing Research & Technology, Kent, WA; [4] Paradigm-ISR, Bend, OR

A paper from the Proceedings of the
13th International Conference on Precision Agriculture
July 31 – August 4, 2016
St. Louis, Missouri, USA

Abstract. *Remote sensing with small unmanned aircraft systems (sUAS) has potential applications in agriculture because low flight altitudes allow image acquisition at very high spatial resolution. We set up experiments at the Oregon State University Hermiston Agricultural Research and Extension Center (HAREC) to assess advantages and disadvantages of sUAS for precision farming. In 2014, we conducted an experiment in irrigated potatoes with 4 levels of artificial infestation by Colorado Potato Beetles. A hexacopter sUAS was flown at two altitudes with a Tetracam Multi Camera Array with 5 bands and one up-looking incident light sensor. After just one day, plant damage was visible, but not correlated with the total number of beetles per plot. Plot-scale spectral vegetation indices, such as NDVI, were not correlated with visible damage. However, the sub-plot area of damage from object-based image analysis was highly correlated. Traditional methods for satellite data may not downscale well for remote sensing from sUAS. Object-based image analysis and computer vision have potential for early detection and reduced cost.*

Keywords. Solanum tuberosum*, Colorado potato beetle,* Leptinotarsa decemlineata, *multi-rotor drone, spectral vegetation indices, object-based image analysis, structure from motion.*

Introduction

Potatoes were the first crop for which insecticides were routinely used (Hare 1990) and potatoes require more pesticides than other major crops (Rondon 2012a,b). Integrated pest management is a collection of methods that consider the whole system to keep insect damage to acceptable levels. Colorado potato beetles (CPB), both larvae and adults, are voracious leaf eaters that can rapidly defoliate a field of potatoes (Hare 1990). Monitoring potato plants for missing leaves and other damage over the growing season is the first step in determining what strategies should be employed for insect control (Rondon 2012a, b).

Monitoring crop production using unmanned aircraft was envisioned long before the technology evolved to make it practical (Jackson & Youngblood 1983). Remote sensing using small unmanned aircraft systems (sUAS) acquires imagery at low altitudes for higher spatial resolution. Remote sensing from sUAS platforms may be ideal for insect pest detection (Yue et al. 2012). What is the best method to analyze high-spatial-resolution imagery in order to detect the presence of potato damage indicating possible infestation by CPB? Traditionally, spectral vegetation indices such as the Normalized Difference Vegetation Index (NDVI, Rouse et al. 1974; Tucker 1979) are correlated with the amount of biomass or damage over some spatial extent. Object-based image analysis (OBIA) capitalizes on high-spatial resolution to group adjacent pixels with similar spectral and textural properties (Laliberte et al. 2004, 2010; Blaschke 2010). More recently, Structure from Motion (SfM) photogrammetry was used to determine plant height, which is often a reliable indicator of growth and biomass (Turner et al. 2012; Westoby et al. 2012; Bendig et al. 2013, 2014).

We set up an experiment in which CPB were added to potato plants to vary the amount of infestation during the vegetative growth stage. The objective was to compare spectral indices, object-based image analysis, and SfM point clouds for early detection of CPB damage.

Methods

The study was conducted at Oregon State University's Hermiston Agricultural Research and Extension Center (HAREC) located in Hermiston, Oregon (45.82021° N and 119.28364° W, at an elevation of 180 m). July is the hottest month with average high and low temperatures of 32° C and 14° C, respectively. The average annual precipitation is 266 mm, with 51 mm during the growing season. The soil type is an Adkins Sandy Loam (coarse-loamy, mixed, superactive, mesic Xeric Haplocalcids).

Small plots (2.6 × 9.2 m) of potatoes (*Solanum tuberosum* L. 'Ranger Russet') were established on 22 April 2014 using a randomized block design with four treatments and four replications (Fig.1A). Irrigation, herbicides, and fungicides were applied in the recommended amounts. Fertilization was about 450 kg/ha nitrogen, 310 kg/ha phosphorus, 220 kg/ha potassium, and 80 kg/ha sulfur. No insecticides were applied.

On 9 June 2014, different numbers of CPB were placed in each plot: low – 1.5 CPB/plant; medium – 4.5 CPB/plant, and high – 7.5 CPB/plant (Fig.1A). The control treatment had no additional CPB, any larvae or adults found in the control plots either emerged from the soil or migrated from other areas. There was no apparent plant damage on 23 June 2014. However, on the next day,24 June 2014,

visual plant damage was obvious. The first CPB population survey was conducted on 2 July 2014.

All sUAS flights were conducted under a Certificate of Authorization from the United States Federal Aviation Administration. A “Spreading Wings” S800 hexacopter (DJI, Shenzhen, Guangdong, China) with a six-band Mini Multi Camera Array (mini-MCA, Tetracam, Inc., Chatworth, CA) was flown over the plots on 10 days in June 2014. The channels were narrow-bands (center wavelength ± 10 nm) in the blue (470 nm), green (550 nm), red (660 nm), red-edge (710 nm), and near-infrared (NIR, 810 nm). The sixth channel was used for an upwards-looking incident light sensor (Heinhold 2014). Using an autopilot, the sUAS flew over the plots first at 60 m and then at 30 m altitude above ground level. The focal length of the Mini-MCA was 9.6 mm, so pixel sizes were about 30 and 15 mm for 60 m and 30 m altitude, respectively.

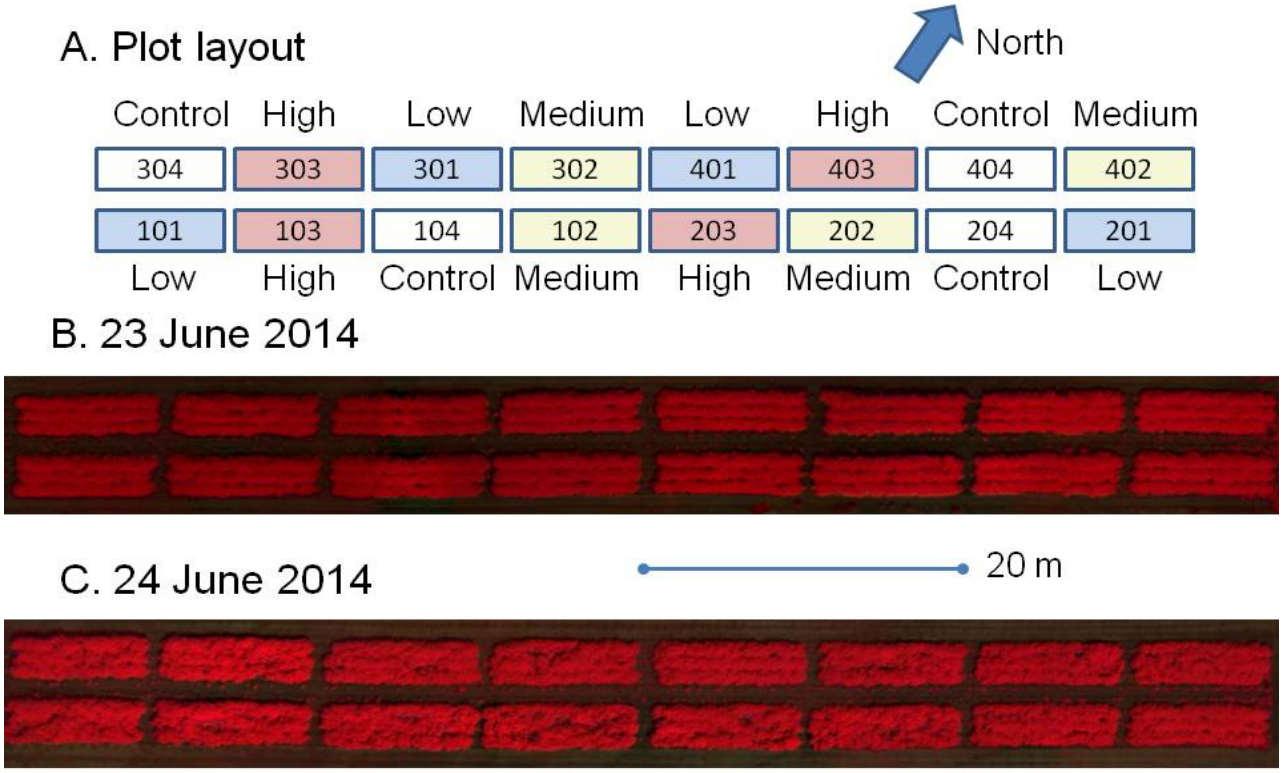

Fig. 1. A. Plot layout for additional Colorado potato beetles (CPB) on ‘Ranger Russet’ potatoes. B. Color-infrared orthomosaic from flights on 23 June 2014 at 60 m agl. C. Color-infrared orthomosaic from flights on 24 June 2014 at 60 m agl.

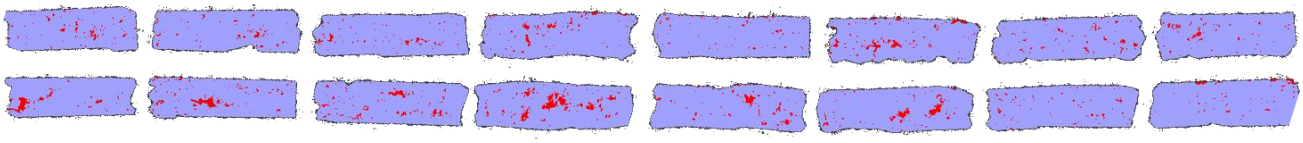

Fig. 2. NDVI feature extraction on 24 June 2014 from images acquired at 30 m altitude. Plots are aligned the same as Fig. 1A. Red areas are defined as CPB damaged.

Only the image data acquired on 23 and 24 June 2014 were analyzed. The images were initially processed using Tetracam’s PixelWrench-2 software to reformat raw imagery to the Tagged Interchange File Format (*.tif) and correct digital numbers to surface reflectance, scaled from 0 to 255. Photoscan Pro (Agisoft, St. Petersburg, Russia) was used to create orthomosaic images and

three-dimensional surface models using the SfM algorithm. Unfortunately, ground control points were not established so the orthomosaics were created only from the sUAS log files. The Environment for Visualizing Images (ENVI) version 5.3 (Excelis Visual Solutions, Harris Corporation, Boulder, CO) was used to calculate spectral vegetation indices and to classify damage with ENVI Feature Extraction based on edge detection. The scale and merge parameters were both 70 to define fewer objects and to more aggressively merge objects, respectively (Fig. 2).

Various spectral indices were calculated; however, results from the different indices were highly correlated. Therefore, only NDVI was used:

$$NDVI = (R_{NIR} - R_R) / (R_{NIR} - R_R) \quad (1)$$

where R_{NIR} = NIR reflectance and R_R = red reflectance (Rouse et al. 1974). A threshold-based estimate of damage was determined for each plot from the percentage of pixels with NDVI ≤ 0.8 from the cumulative NDVI frequency distribution. Spearman rank correlation coefficients (r_s) were calculated and *t*-tests were used to determine significance (Steel and Torrie 1960).

Results and Discussion

There was no indication of potato leaf loss or plant damage from the images acquired on 23 June 2014 (Fig. 1B). There were visibly-damaged areas in all plots on the very next day (Fig. 1C). The least impacted plots were 201 and 401, and the most impacted plot was 202 (Fig. 1C). The number of CPB found in each plot on the first census and a visual ranking of damage (least to most) were not related to the numbers of artificially applied CPB from the experimental treatments (data not shown).

There was no relationship (r_s = 0.00) between the visual damage ranking and CPB numbers in each plot (Fig. 3A). Also, plot average NDVI was not related (r_s = 0.23) to the visual ranking of damage (Fig. 3B). Mean NDVI was high for all plots at both 30 m and 60 m altitudes with a narrow range of 0.85 to 0.90 (Fig. 3B). A threshold of NDVI ≤ 0.80 was determined for classification of damage/no damage, because the resulting spatial patterns of pixels classified as damaged were similar to the spatial patterns of damage from visual assessment.

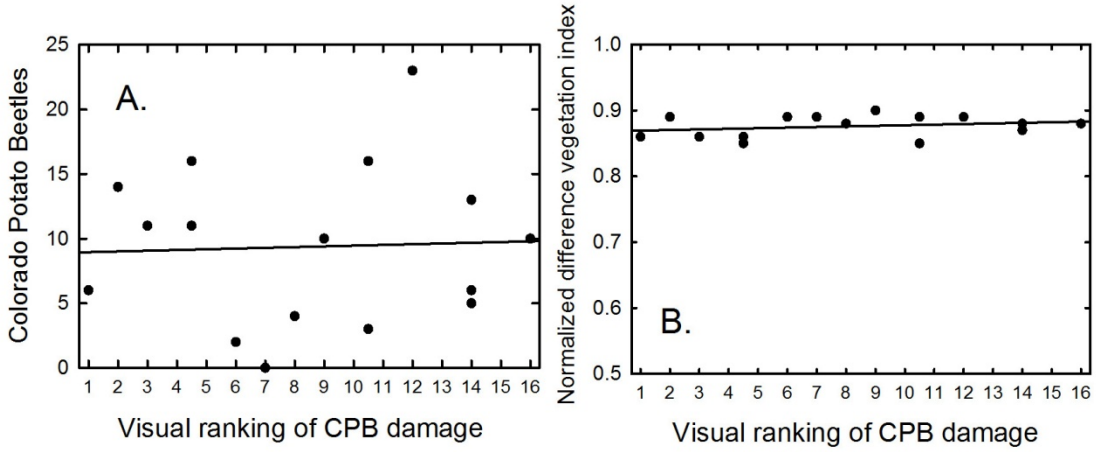

Fig. 3. CPB damage per plot was ranked from least to most. A. The number of CPB counted per plot on 2 July 2014. B. Plot-mean NDVI on 24 June 2014 from an altitude of 30 m.

However, the number of pixels classified as damaged from an NDVI threshold was not related (r_s = 0.27) to the visual ranking of CPB damage (Fig. 4A). Image objects defined by edge features were classified as damaged if the object's NDVI ≤ 0.80 (Fig. 4B). The ranking of visual damage was highly

correlated to the plot object area classified as damaged (r_s = 0.85, t = 6.08 with 14 degrees of freedom).

The difference between classifications using an NDVI threshold (Fig. 4A) and using objects from NDVI feature extraction (Fig. 4B) may not be important depending on the objective. If detection of plant damage and its location was the goal, then the NDVI threshold would be sufficient, because the threshold was selected based on the visual spatial paterns. However, if the area of damage is used to trigger different options available from Integrated Pest Management, then feature extraction methods would have to be considered.

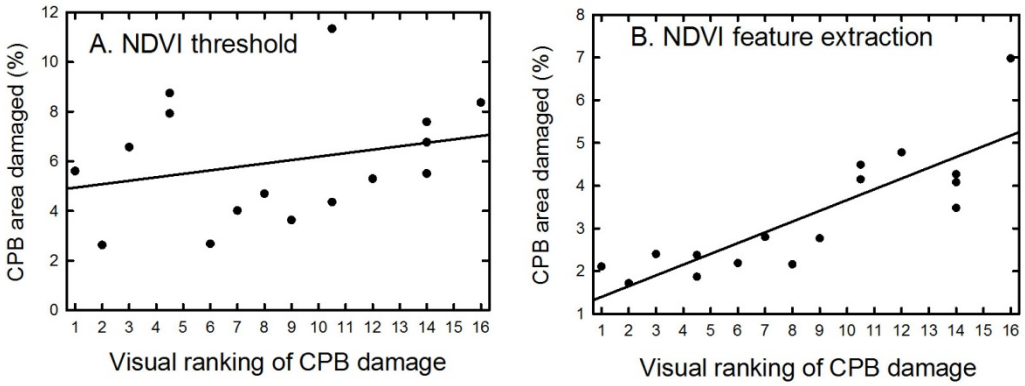

Fig. 4. Analysis of the 24 June 2014 images from an altitude of 30 m: A. Area (% of plot) classified with CPB damage using an NDVI threshold of ≤ 0.80. B. Object area classified with CPB damage using feature extraction of the NDVI image.

.

For the most impacted plot (202, Fig. 1A), the area classified as damaged was less than 10%, which was too small to affect plot mean NDVI. Based on the plot area, an equivalent satellite pixel size would be about 5 m; the NDVI values (Fig. 3B) suggest that multispectral satellite with this pixel size would not detect the changes that occurred over the 1 day (0.1 area × 0.6 NDVI + 0.9 area × 0.9 NDVI = 0.87). Hunt et al. (2007) used models and hyperspectral data from the Airborne Visible Infrared Imaging Spectrometer to determine that an area of at least 10% is needed to detect the spectrally-distinct flower bracts of leafy spurge by spectral unmixing using the Spectral Angle Mapper. Therefore, there is say a 50:50 chance that hyperspectral sensors with 5-m pixel sizes would not have detected the area damaged by CPB. As the 2014 growing season progressed, CPB damage accumulated to over 75% of the area in each plot. At such high levels of damage, it is likely that any method of remote sensing would have been successful.

Structure from motion point clouds are intermediate photogrammetric products from orthomosaicing numerous overlapping images (Turner et al. 2012; Westoby et al. 2012). With higher spatial resolution available from low-altitude sUAS, digital surface models show spatial variations in plant height (Bendig et al. 2013, 2014). We constructed four digital surface models (2 dates × 2 altitudes) from sUAS point clouds and found that depressed areas in Fig. 5B corresponded with areas of CPB damage in Fig. 1C. In this experiment however, the quantitative information on plant height was not accurate because the digital surface models had overall features not related to the flat soil surface. There was an overall convex shape in Fig. 5A and an overall concave shape in Fig. 5B. From Agisoft LCC support personnel, the most likely reason for the overall shapes was that we did not place visible ground control points in the experimental study area. Currently, there are substantial costs for: (1) acquiring dense coverage of aerial images from sUAS and (2) for computer processing. Therefore, acquiring and processing SfM point clouds may be too expensive for some applications.

There are many options in workflows for acquiring and analyzing sUAS imagery (Torres-Sánchez et

al. 2013; Mathews 2014; Salamí et al. 2014). For determining in-season nitrogen fertilizer requirements, Hunt et al. (2014) suggested that transects of single images over large fields would be most cost effective, because variation of fertilizer requirements is largely caused by variation in soil properties. Each image should have ultra-high spatial resolution to determine plant cover and chlorophyll content of single leaves. With insect pests, the pattern of damage is unpredictable, so frequent, continuous coverage may be required. However, if the spatial distribution of damage is clumped (as in Fig. 2), then pixel sizes could be somewhat larger and would still be effective.

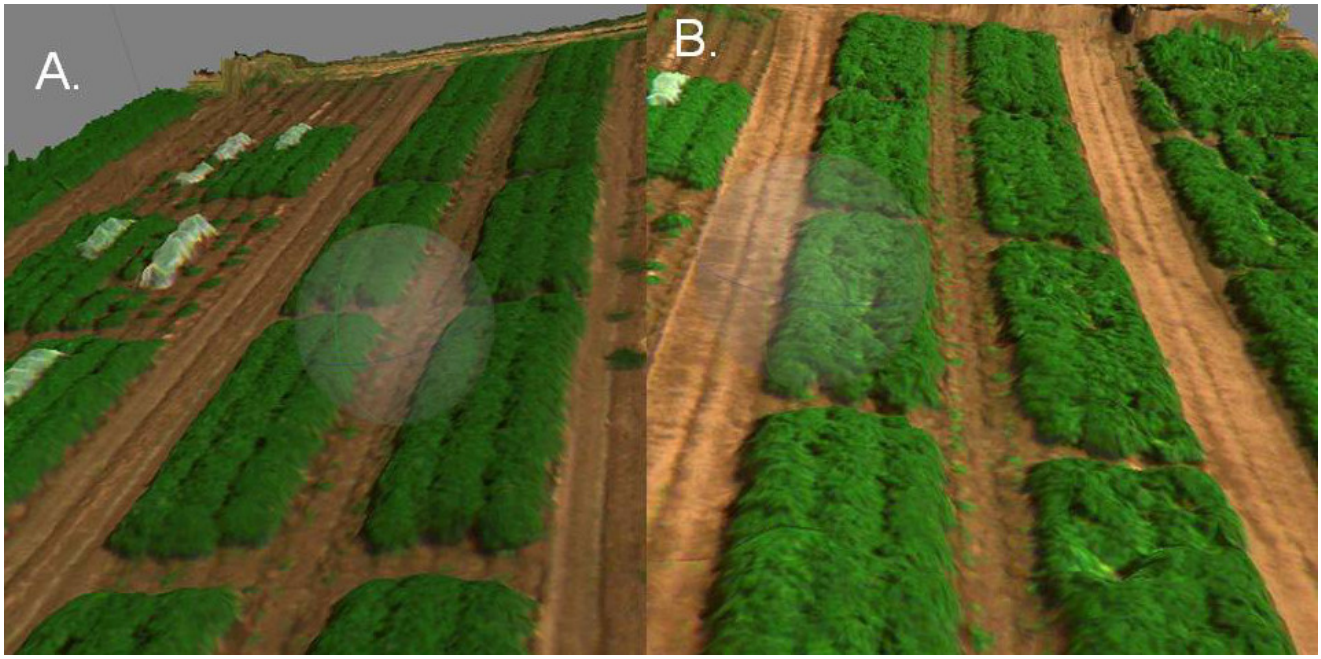

Fig. 5. True-color SfM perspectives looking north-east on A. 23 June 2014 and B. 24 June 2014. Damage from CPB created depressions in the canopy surface model. Altitude of sUAS was 30 m.

Conclusions

Leaf and plant damage caused by Colorado potato beetles was spatially unpredictable and appeared just over one day, so frequent sUAS flights with extensive coverage were needed for early detection. Based on calculations and ignoring problems with cloud cover, satellite data with 5-m pixels would not be effective for monitoring CPB damage. Feature extraction based on object-based image analysis was the most accurate method for detecting the area with plant damage; however, this method required extensive operator intervention for success. We are intrigued by the potential using plant height from SfM point clouds, because undamaged plants could serve as field-by-field references to determine relative heights for damage assessment.

Acknowledgements

Project was funded in part by Boeing Research & Technology, Kent, WA. We thank Philip B. Hamm for facilitating the research at the Hermiston Agricultural Research and Extension Center.

References

Bendig, J., Bolten, A. & Bareth, G. (2013). UAV-based imaging for multi-temporal, very high resolution crop surface models to monitor crop growth variability monitoring. *Photogrammetrie Fernerkundung Geoinformation*, 6, 551-562.

Bendig, J., Bolten, A., Bennertz, S., Broscheit, J., Eichfuss, S., & Bareth, G. (2014). Estimating biomass of barley using crop surface models (CSMs) derived from UAV-based RGB imaging. *Remote Sensing*, 6, 10395-10412.

Blaschke, T. (2010). Object based image analysis for remote sensing. *ISPRS Journal of Photogrammetry and Remote Sensing*, 65, 2-16.

Hare, J. D. (1990). Ecology and management of the Colorado potato beetle. *Annual Review of Entomology*, 35, 81-100.

Heinhold, S. (2014). Radiometric multi-spectral or hyperspectral camera array using matched area sensors and a calibrated ambient light collection device. United States Patent US 2014/0022381 A1.

Hunt, E. R., Jr., Daughtry, C. S. T., Kim, M. S., & Parker Williams, A. E. (2007). Using canopy reflectance models and spectral angles to assess potential of remote sensing to detect invasive weeds. *Journal of Applied Remote Sensing*, 1, 013506, DOI: 10.1117/1.2536275.

Hunt, E. R., Jr., Daughtry, C. S. T., Mirsky, S. B., and Hively, W. D. (2014). Remote sensing with simulated unmanned aircraft imagery for precision agriculture applications. *IEEE Journal of Selected Topics in Applied Earth Observations and Remote Sensing*, 7, 4566-4571.

Jackson, R. D. & Youngblood, J. W. (1983). Agriculture's eye in the sky. Forever plane could give continuous crop data. *Crops and Soils Magazine*, October, 15-18.

Laliberte, A., Herrick, J. E., Rango, A., & Winters, C. (2010). Acquisition, orthorectification, and object-based classification of unmanned aerial vehicle (UAV) imagery for rangeland monitoring. *Photogrammetric Engineering & Remote Sensing*, 76, 661-672.

Laliberte, A. S., Rango, A., Havstad, K. M., Paris, J. M., Beck, R. F., McNeely, R., & Gonzalez, A. L. (2004). Object-oriented image analysis for mapping shrub encroachment from 1937 to 2003 in southern New Mexico. *Remote Sensing of Environment*, 93, 198-210.

Mathews, A. J. (2014). Object-based spatiotemporal analysis of vine canopy vigor using an inexpensive unmanned aerial vehicle remote sensing system. *Journal of Applied Remote Sensing*, 8, 085199-1, DOI: 10.1117/1.JRS.8.085199.

Rondon, S. I. (2012a). Building and Integrated Pest Management for Potatoes In North America: Where to Start? *Acta Horticulturae*, 960, 371-384. DOI: 10.17660/ActaHortic.2012.960.54

Rondon, S. I. (2012b). Pest management strategies for potato insect pests in the Pacific Northwest of the United States. In F. Perveen (Ed.), *Insecticides – Pest Engineering* (309-332). Rijeka, Croatia: InTech. http://cdn.intechopen.com/pdfs/28267.pdf

Rouse, J. W., Haas, R. H., Schell, J. A., & Deering D. W. (1974). Monitoring vegetation systems in the Great Plains with ERTS. In *Third Earth Resources Technology Satellite-1 Symposium*, Volume 1, (309-317). NASA SP-351, Washington, DC: National Aeronautics and Space Administration.

Salamí, E., Barrado, C., & Pastor, E. (2014). UAV flight experiments applied to the remote sensing of vegetated areas. *Remote Sensing*, 6, 11051-11081.

Steel, R. G. D. and Torrie, J. H. (1960). *Principles and Procedures of Statistics.* New York: McGraw-Hill.

Tucker, C. J. (1979). Red and photographic infrared linear combinations for monitoring vegetation. *Remote Sensing of Environment*, 8, 127-150.

Turner, D., Lucieer, A., & Watson, C. (2012). An automated technique for generating georectified mosaics from ultra-high resolution unmanned aerial vehicle (UAV) imagery, based on structure from motion (SfM) point clouds. *Remote Sensing*, 4, 1392-1410.

Westoby, M. J., Brasington, J., Glasser, N. F., Hambrey, M. J. & Reynolds, J. M. (2012). 'Structure-from-Motion' photogrammetry: A low-cost, effective tool for geoscience applications. *Geomorphology*, 179, 300-314.

Yue, J., Lei, T., Li, C., & Zhu, J. (2012). The application of unmanned aerial vehicle remote sensing in quickly monitoring crop pests. *Intelligent Automation and Soft Computing*, 18, 1043-1052.